Decoherence and Mode Hopping in a Magnetic Tunnel Junction Based Spin Torque Oscillator

P. K. Muduli,[1] O. G. Heinonen,[2,3] and Johan Åkerman[1,4]

[1]*Physics Department, University of Gothenburg, 41296 Gothenburg, Sweden*
[2]*Materials Science Division, Argonne National Laboratory, Lemont, Illinois 60439, USA*
[3]*Department of Physics and Astronomy, Northwestern University, 2145 Sheridan Road, Evanston, Illinois 60208-3112, USA*
[4]*Materials Physics, School of ICT, KTH-Royal Institute of Technology, Electrum 229, 164 40 Kista, Sweden*

We discuss the coherence of magnetic oscillations in a magnetic tunnel junction based spin torque oscillator as a function of the external field angle. Time-frequency analysis shows mode hopping between distinct oscillator modes, which arises from linear and nonlinear couplings in the Landau-Lifshitz-Gilbert equation, analogous to mode hopping observed in semiconductor ring lasers. These couplings and, therefore, mode hopping are minimized near the current threshold for the antiparallel alignment of free-layer with reference layer magnetization. Away from the antiparallel alignment, mode hopping limits oscillator coherence.

Magnetization precession at GHz frequencies can be sustained in spin-valve and magnetic tunnel junction (MTJ) based spin-torque oscillators (STOs) by directly transferring spin angular momentum from spin polarized current [1,2] to the free-layer magnetization order parameter. A fundamental question is the stochastic phenomena that govern its coherence time (τ_c). Theoretical studies [3,4] have investigated decoherence through thermal noise, assuming that only a single mode is excited. Other theoretical works conclude that only the lowest energy mode supports sustained oscillations [5]. Yet experiments clearly show the existence of multiple modes in spin valves [6–9] and MTJs [10–14], and persistent mode hopping [8,9] between several modes. The impact on τ_c of such mode hopping is largely unexplored, and theoretical investigations of its origin are entirely lacking.

Here we present systematic experimental investigations into mode hopping and its impact on coherence time, as functions of current and applied field angle in MTJ-STOs. We derive equations showing how such systems are analogous to semiconductor ring lasers and under driving can exhibit mode hopping in the presence of stochastic noise. Nonconservative torques in the Landau-Lifshitz equation couple individual modes. The coupling has a minimum when the nonconservative torques cancel each other, explaining the experimentally observed suppression of mode hopping at angles near (but not exactly at) antiparallel (AP) alignment. Micromagnetic simulations of magnetization dynamics support this picture. Finally, we show that although mode hopping is the limiting factor for STO coherence at most angles, single-mode nonlinear spin-torque auto-oscillator (NSTO) theory [3] qualitatively holds when dwell time is sufficiently large compared with the oscillations' coherence time.

The MTJ nanopillars used in this work are similar to those in Ref. [14]. The layer structure consists

of IrMn(5)/CoFe(2.1)/Ru(0.81)/CoFe(1)/CoFeB(1.5)/ MgO(1)/CoFeB(3.5) (thickness in nm), where the bottom CoFe layer is the pinned layer, the composite CoFe/CoFeB represents the reference layer (RL), and the top CoFeB layer is the free layer (FL). We discuss results from a *circular* device with approximate diameter 240 nm, resistance-area product 1.5 $\Omega \, \mu m^2$, and tunneling magnetoresistance 75%. The RL magnetization equilibrium direction is along the positive $\hat{x}$ direction, which is also 0° of the applied field. We use the convention that a positive current flows from the FL to the RL.

Figure 1(a) shows the resistance R as a function of the in-plane angle φ of applied field H. Here we focus on magnetic excitations with $H = 450$ Oe and $140° \leq \varphi \leq 220°$, for which the FL rotates *coherently* with the field [Fig. 1(a)]; with a positive current, FL modes are excited. In general, several modes are found in frequency-domain measurements, and we have identified five potential FL modes ($m_i, i = 1, \ldots, 5$) [14] from measurements at 8 mA. These modes' frequencies decrease when the field angle
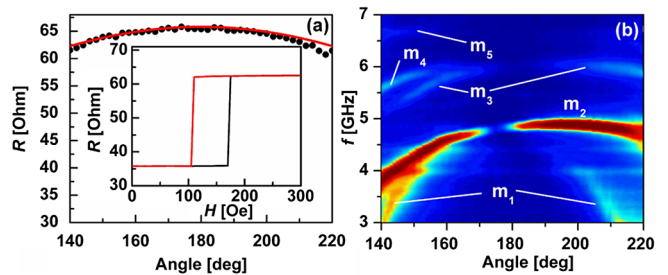

FIG. 1 (color online). (a) Experimental (circles) and calculated (solid line) resistance versus the in-plane field angle φ at $H = 450$ Oe; $\varphi = 180°$ corresponds to AP alignment of FL and RL. Inset: Magnetoresistance loop measured at $\varphi = 180°$. (b) Map of power (dB) vs frequency (f) and φ for $I = 8$ mA and $H = 450$ Oe.

moves away from 190°, and are asymmetric about their maxima. Both the decrease and asymmetry are unexpected from a simple Kittel formula [14], in which ferromagnetic coupling between the FL and RL would result in mode frequencies symmetric at about 180° and frequency minima at 180°.

In order to quantitatively analyze the STO's time-frequency behavior, we collected 1000 ns-long time traces [15] of the STO voltage signal at different field angles and bias currents. Figure 2 shows the frequency vs time obtained from Wigner transforms of the traces at three representative angles, $\varphi = 140°$, 196°, and 220°, and at 8 mA using a time (frequency) resolution of 1.25 ns (0.8 GHz). We chose these angles because at 140° and 220° the FL and RL are far from their AP configuration, but the FL still rotates coherently with the external field, and at 196° we observed the longest coherence time of mode m_2, because of the device's slight asymmetry [Fig. 1(b)] and because, closer to 180°, the observed m_2 coherence time is limited by frequency doubling [11,16]. The plots in Fig. 2 show that for 196°, the STO mostly stays in mode m_2. In contrast, frequent mode hopping occurs between m_1 and m_2 at 220°, and between m_1, m_2, and m_4 at 140°. We note that this mode hopping behavior between distinct STO modes differs from the observations in Ref. [17], where the dominant mode's frequency fluctuated in time, on the scale at ~0.01 GHz. A detailed examination of time-frequency plots shows that mode hopping occurs at all field angles and currents [15], and is completely random in time. The central mode m_2 is the most stable at all angles; spin-torque preferentially excites mode m_2.

The coherence time of mode m_2 can be obtained by autocorrelating time traces. The right side of Fig. 2 shows the traces' normalized autocorrelation function, $\Gamma(\tau)$, filtered in a range of -300 MHz/ $+400$ MHz around m_2.

This filter width avoids overlapping other modes. The autocorrelation functions decay exponentially in time, which is consistent with thermally activated stochastic processes leading to decoherence [18]. The corresponding decay time τ_c, which is the coherence time for m_2, was obtained by fitting $\Gamma(\tau)$ to a function of the form $e^{-\tau/\tau_c}$. We can compare τ_c with the average dwell time t_{ave} in mode m_2, which is obtained by analyzing the instantaneous STO frequency [15]. Figure 3 shows the central experimental result: τ_c and t_{ave} as functions of current at 140°, 196°, and 220°. Both τ_c and t_{ave} depend on the field angle and current. At 196°, t_{ave} exceeds τ_c by over an order of magnitude for currents in a range about the threshold current. Here, mode hopping is insignificant and does not limit coherence, the STO has a well-defined single mode, and we show below that NSTO theory applies here. For 140° and 220°, τ_c and t_{ave} are approximately equal (within experimental uncertainty in t_{ave} [15]). Here, mode hopping limits coherence time; more extensive analysis shows that for $\varphi \lesssim 165°$ and $\varphi \gtrsim 205°$, mode hopping is the dominant decoherence process.

We now discuss the experimental results. The magnetization dynamics can be described by the Landau-Lifshitz-Gilbert (LLG) equation, which we write as

$$\frac{d\hat{m}}{dt} = -\hat{m} \times [\mathbf{H}_0 + \mathbf{h}_d]$$
$$- \alpha\hat{m} \times \left\{ \hat{m} \times \left[\mathbf{H}_0 - \frac{a_J}{\alpha}\mathbf{M} \right] + \hat{m} \times \mathbf{h}_d \right\},$$

where $\hat{m}(\mathbf{r})$ is the local magnetization direction of the FL and $\mathbf{M}$ is that of the RL; $\mathbf{H}_0$ is the total *static* effective field, including the out-of-plane spin-torque; $\mathbf{h}_d$ is the *dynamic* demagnetizing field arising from the oscillating magnetization density in FL; a_J is the in-plane effective field due to spin-torque; and α is the dimensionless damping. First, micromagnetic simulations confirm that the asymmetry in mode frequencies of about $\varphi = 180°$ [Fig. 1(b)] can be
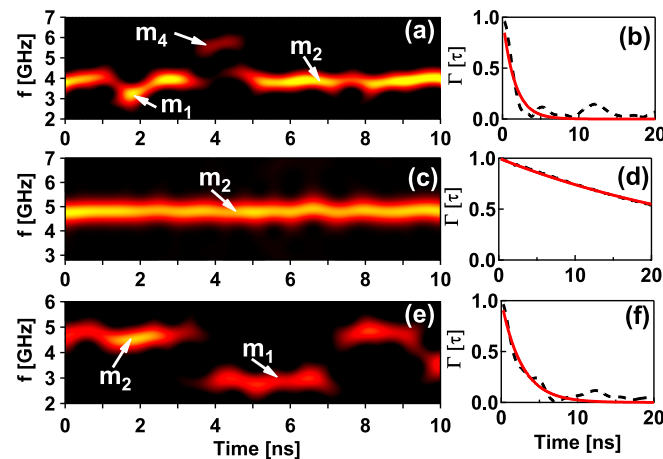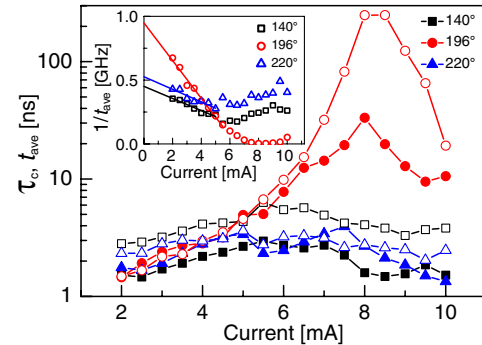

FIG. 2 (color online). Wigner distribution (first column), and normalized autocorrelation envelope (second column) at (a), (b) 140°, (c), (d) 196°, and (e), (f) 220° for $I = 8$ mA and $H = 450$ Oe. Red lines are exponential fits to experimental autocorrelation envelope (dashed lines).

FIG. 3 (color online). Coherence time τ_c (filled symbols) and average dwell time t_{ave} (open symbols) vs I at 140° (black squares), 196° (red circles), and 220° (blue triangles). Inset: Corresponding $1/t_{ave}$ vs I showing a clear angular dependence of $1/t_{ave}$ for $I \to 0$.

caused by small ellipticity in the structure, with the exchange bias slightly misaligned with the major axis, as the resonance modes are sensitive to the equilibrium magnetization details. The magnetoresistance, however, remains nearly symmetric at about $\varphi = 180°$, as it measures the *average* angle between RL and FL magnetization directions. Now consider a system with the equilibrium FL magnetization along $\mathbf{H}_0$, which is at an angle ϕ to the applied field. The linearized (about static equilibrium) LLG equation can be recast as an eigenvalue equation $\mathcal{L}(\mathbf{r}, \mathbf{r}'; \omega)\hat{m}(\mathbf{r}') = 0$. At zero damping and current, all torques in the LLG equation are conservative, and the eigenvalues are real and undamped, but finite damping or current gives rise to nonconservative torques, and eigenvalues become complex. We now outline how this leads to mode coupling [15]. We restrict the discussion to two modes, and write the magnetization texture as $\hat{m}(\mathbf{r}, t) = c_1(t)\hat{m}_1(\mathbf{r})e^{-i\omega_1 t} + c_2(t)\hat{m}_2(\mathbf{r})e^{-i\omega_2 t}$, where $\hat{m}_i(\mathbf{r})$ is an eigenmode of the *linearized* LLG with eigenfrequency ω_i; the coefficients c_i carry the slow time dependence (on observational time scales τ_{obs}) of the magnetization texture. We insert this into the full nonlinear LLG, project onto $\hat{m}_i$, and average over fast time scales, before expanding the nonlinear projections in c_i. We write the result as

$$\dot{c}_1 = -i[\omega_1 \eta_{1,1}|c_1|^2 + \omega_2 \eta_{1,2}|c_2|^2]c_1$$
$$\quad - \Gamma_G[1 + P_{1,1}\omega_1|c_1|^2 + P_{1,2}\omega_2|c_2|^2]c_1$$
$$\quad + \sigma_0 I[1 - Q_{1,1}\omega_1|c_1|^2 - Q_{1,2}\omega_2|c_2|^2]c_1 + R_{1,2}c_2,$$
$$\dot{c}_2 = -i[\omega_1 \eta_{2,1}|c_1|^2 + \omega_2 \eta_{2,2}|c_2|^2]c_2$$
$$\quad - \Gamma_G[1 + P_{2,1}\omega_1|c_1|^2 + P_{2,2}\omega_2|c_2|^2]c_2$$
$$\quad + \sigma_0 I[1 - Q_{2,1}\omega_1|c_1|^2 - Q_{2,2}\omega_2|c_2|^2]c_2 + R_{2,1}c_1,$$

where $\eta_{i,j}$, $P_{i,j}$, and $Q_{i,j}$ are real; $R_{i,j}$ is complex. The factors $\eta_{i,j}$ are nonlinear frequency shifts, $P_{i,j}$ is the nonlinear positive damping, $Q_{i,j}$ is the nonlinear negative damping, and σ_0 is the usual spin-torque coefficient defined in Ref. [6]. These equations are generalizations of the equation for the single-mode NSTO [3]. We note the linear "backscattering" term $R_{1,2}$ ($R_{2,1}$) in these equations. This term does not appear in normal spin-wave expansions of Hamiltonians or equations of motion as it violates energy conservation on short time scales. Here, however, we consider conditions close to threshold: Energy is approximately conserved on long time scales, and we enforce the constraint $\omega_1|c_1|^2 + \omega_2|c_2|^2 = p$, where p is a constant. On general grounds, we can set $Q_{1,2} = Q_{2,1} = Q_0$, $P_{1,2} = P_{2,1} = P_0$, and $R_{1,2} = R_{2,1} = u + iv$. We introduce new variables $Q_i e^{i\phi_i} = \sqrt{\omega_i}c_i$ and $\psi = \phi_2 - \phi_1$ and use the constraint $Q_1\dot{Q}_1 + Q_2\dot{Q}_2 = 0$. The equations for slow time evolution can then be recast as a two-dimensional Z_2-invariant dynamical system, analogous to that describing semiconductor ring lasers [19,20]. Close to threshold, these equations are known [20] to have two

stable solutions (either of the two modes) close to a homoclinic bifurcation. In the presence of a stochastic field originating from, e.g., contact with a thermal bath, competition between linear and nonlinear couplings can lead to mode hopping [19–21] between the two stable solutions. Nonconservative torques lead to linear and nonlinear couplings between modes, as expressed by the terms in $Q_{i,j}$, $P_{i,j}$, and $R_{i,j}$, $i \neq j$. As the bias current increases from zero, the local nonconservative field is $\alpha\hat{m} \times [\mathbf{H}_0 - \frac{a_J}{\alpha}\mathbf{M}]$; this field also dominates the damping (imaginary parts of eigenvalues). For arbitrary field angles, a current exists—the threshold current—at which the energy dissipation rate equals the rate at which energy is pumped into the system by the spin torque. At this current, energy conservation $Q_1^2 + Q_2^2 = 0$ is strict, but the couplings between modes do not vanish, and the system exhibits mode hopping: the system's total energy is conserved, but energy is transferred back and forth between the modes. However, at 180°, $\mathbf{H}_0$ and $\mathbf{M}$ are collinear, and at threshold energy dissipation equals energy pumping *and* local dissipative torques vanish. Ignoring the nonlocal dissipative torques, this means that *all* terms multiplying Γ_G, $\sigma_0 I$, as well as $R_{i,j}$, vanish. Consequently, mode hopping is minimized. The system's total energy is conserved, and each mode's energy is also individually conserved.

Figure 4 shows Wigner transforms of magnetization time traces obtained from micromagnetic modeling for a system similar to the experiment [15]. At a finite temperature of $T = 300$ K and $I = 8$ mA, mode hopping occurs at 140°, while at 180° precession is coherent at the m_2 mode—this current is just above the threshold for this field angle. Yet at $T = 0$ K, no mode hopping occurs. Apart from demonstrating that mode hopping exists within the micromagnetic model, the modeling shows that (a) mode hopping is induced by thermal fluctuations, and (b) the angle dependence of mode hopping agrees qualitatively with our analysis above.

If the mode resident time t_{ave} is long enough, one can analyze the system in terms of single-mode NSTO theory [6]. The experimental coherence time τ_c can then be
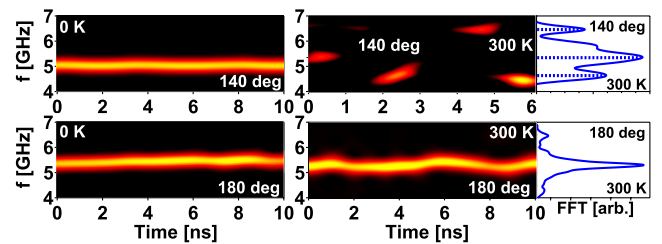

FIG. 4 (color online). Wigner transforms of micromagnetic time traces of average FL magnetization at $T = 0$ K (left) and $T = 300$ K (middle). The right side represents the Fourier transform (FFT) of the 100 ns-long time trace at 300 K. The top row is for 140°; the bottom row is for 180°. The bias current was 8 mA.

compared with that from NSTO theory. Under the assumption that $\tau_c \propto 1/\Delta f$, with Δf the linewidth, we plot $1/(\pi\tau_c)$ against the bias current and fit $1/(\pi\tau_c)$ to the NSTO expression [6] for the subthreshold linewidth, $\Delta f = \Gamma_G(1 - I/I_{th})$, where Γ_G is the natural FMR linewidth, and I_{th} is the threshold current [Fig. 5(a)]. For 196°, we obtain $\Gamma_G \approx 300$ MHz and $I_{th} = 6.4$ mA. This Γ_G is comparable to previous reports [22] and agrees well with an estimate using these material parameters for FL: saturation magnetization $M_0 = 1000$ emu/cm^3, Gilbert damping parameter $\alpha_G = 0.01$. Above $I_{th} = 6.4$ mA, $1/(\pi\tau_c)$ increases with current, qualitative agreeing with the NSTO theory prediction. Thus, the linewidth from NSTO theory qualitative describes $1/(\pi\tau_c)$ at 196° [15]. This is consistent with t_{ave} being large enough that the linewidth is well described by decoherence caused by single-mode thermal fluctuations. However, for 140° and 220°, the coherence is now limited by mode hopping, and we show that the strong increase of $1/(\pi\tau_c)$ above 8 mA is primarily due to increased mode hopping, not due to increased nonlinearity in NSTO theory.

Figure 5(c) shows the measured power restoration rate Γ_p [23]. According to NSTO theory, Γ_p vanishes as $\Gamma_G(I/I_{th} - 1)$ near the threshold. Again, for 196° the agreement between the measured power restoration rate and the NSTO theory prediction is reasonably good. But for 140° and 220°, the power restoration rates, like the linewidths, have much larger minimum values, which is consistent with a limiting decoherence process other than thermal fluctuations at about m_2. We note that even for 196°, Γ_p does not vanish at $I = I_{th}$, indicating either non-

zero mode hopping or the presence of additional sources of noise. Further inconsistencies between NSTO theory and experimental data are provided by the power distribution functions shown on the right side of Fig. 5. The current values are chosen such that $I/I_{th} = 1.25$ in all cases. According to NSTO theory, the power distribution function $\mathcal{P}(p)$ has the form of a Gaussian [24] $\exp[-(p-p_0)^2/2\Delta p^2]$ for $I > I_{th}$, where p_0 denotes stationary power and Δp denotes the power fluctuations. This agrees well with the measured power distribution function near $\varphi = 196°$, shown by the solid line in Fig. 5(d), with the relative power fluctuations $\Delta p/p_0$ in the 0.2–0.4 range, similar to that obtained in Ref. [25]. In contrast, the power distributions are exponential at 140° and 220°, which is consistent with below-threshold conditions. We conclude that the threshold currents for these angles extracted from the linewidth measurements using NSTO theory are too small. Consequently, the increase in measured linewidth $1/(\pi\tau_c)$ above 8 mA at 140° and 220° *cannot* be attributed to an increase in nonlinearity, unlike Ref. [22]. This is further supported by the fact that the experimental nonlinear frequency shift did not show any strong angular dependence [15].

One can qualitatively understand how moderate mode hopping changes NSTO theory. First, it leads to effectively increased power dissipation from mode m_2, since hopping decreases the power in this mode. Second, for short excursions to other modes, the oscillator phase is random as it returns to m_2, and is not correlated with the phase before the excursion. This means mode hopping adds extra phase noise to oscillators. Within this simple picture, we write the expression for the subthreshold linewidth as $\Delta f \approx \Gamma_G - \sigma_0 I + \frac{a}{t_{ave}}$; a is a dimensionless constant of order unity. Since a/t_{ave} depends on the angle for $I \rightarrow 0$ (see Fig. 3, inset), this explains the obtained apparent angular dependence of the zero-current linewidth Γ_G [Fig. 5(a)]. Furthermore, the extrapolated threshold current value shifts to a larger value, the shift being larger for weaker current-dependence of t_{ave}, consistent with a larger threshold current for 140° and 220° than that extrapolated using NSTO theory.

In summary, we have observed and analyzed multimode excitations and mode hopping in an MgO-based STO. Mode hopping occurred at all angles and currents, contrary to two-mode theory [5] and expectations [3]. Insofar as the basic physics of mode hopping appears to be intrinsic to the LLG equations governing the dynamics of the oscillator nanosized systems with single-domain equilibrium magnetization, efforts to reduce decoherence may need to focus on better understanding the energy barrier separating stable modes.
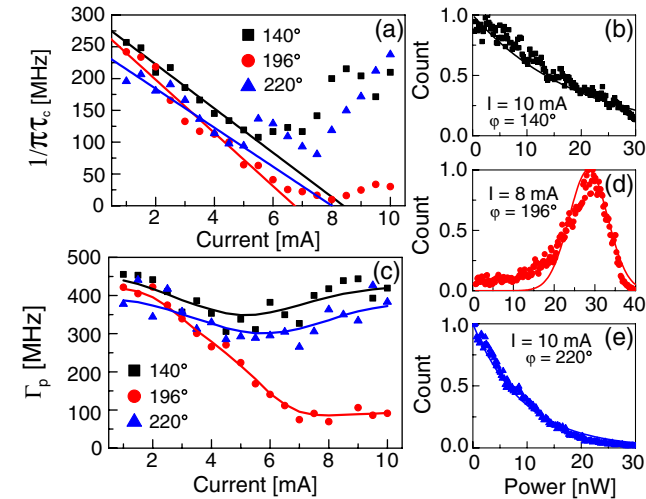
FIG. 5 (color online).   (a) $1/(\pi\tau_c)$ vs current at 140° (black squares), 196° (red circles), and 220° (blue triangles). Solid lines are fits to the subthreshold region; intercepts with the horizontal axis indicate threshold currents. (c) Power restoration rate Γ_p vs current at 140° (black squares), 196° (red circles), and 220° (blue triangles). Solid lines are visual guides. Right: Normalized power distribution function and fits at (b) 140°, (d) 196°, and (e) 220°.

PHYSICAL REVIEW LETTERS

---

[1] J. C. Slonczewski, J. Magn. Magn. Mater. **159**, L1 (1996); L. Berger, Phys. Rev. B **54**, 9353 (1996).

[2] M. Tsoi, A. G. M. Jansen, J. Bass, W.-C. Chiang, V. Tsoi, and P. Wyder, Nature (London) **406**, 46 (2000); S. I. Kiselev, J. C. Sankey, I. N. Krivorotov, N. C. Emley, R. J. Schoelkopf, R. A. Buhrman, and D. C. Ralph, *ibid.* **425**, 380 (2003).

[3] J.-V. Kim, V. Tiberkevich, and A. N. Slavin, Phys. Rev. Lett. **100**, 017207 (2008); J.-V. Kim, Q. Mistral, C. Chappert, V. S. Tiberkevich, and A. N. Slavin, *ibid.* **100**, 167201 (2008); A. Slavin and V. Tiberkevich, IEEE Trans. Magn. **45**, 1875 (2009).

[4] T. Silva and M. Keller, IEEE Trans. Magn. **46**, 3555 (2010).

[5] F. M. de Aguiar, A. Azevedo, and S. M. Rezende, Phys. Rev. B **75**, 132404 (2007).

[6] S. I. Kiselev, J. C. Sankey, I. N. Krivorotov, N. C. Emley, M. Rinkoski, C. Perez, R. A. Buhrman, and D. C. Ralph, Phys. Rev. Lett. **93**, 036601 (2004).

[7] J. C. Sankey, I. N. Krivorotov, S. I. Kiselev, P. M. Braganca, N. C. Emley, R. A. Buhrman, and D. C. Ralph, Phys. Rev. B **72**, 224427 (2005).

[8] I. N. Krivorotov, N. C. Emley, R. A. Buhrman, and D. C. Ralph, Phys. Rev. B **77**, 054440 (2008).

[9] S. Bonetti, V. Tiberkevich, G. Consolo, G. Finocchio, P. Muduli, F. Mancoff, A. Slavin, and J. Åkerman, Phys. Rev. Lett. **105**, 217204 (2010).

[10] A. V. Nazarov, K. Nikolaev, Z. Gao, H. Cho, and D. Song, J. Appl. Phys. **103**, 07A503 (2008).

[11] A. M. Deac, A. Fukushima, H. Kubota, H. Maehara, Y. Suzuki, S. Yuasa, Y. Nagamine, K. Tsunekawa, D. D. Djayaprawira, and N. Watanabe, Nature Phys. **4**, 803 (2008).

[12] D. Houssameddine, S. H. Florez, J. A. Katine, J.-P. Michel, U. Ebels, D. Mauri, O. Ozatay, B. Delaet, B. Viala, L. Folks, B. D. Terris, and M.-C. Cyrille, Appl. Phys. Lett. **93**, 022505 (2008).

[13] Z. Zeng, K. H. Cheung, H. W. Jiang, I. N. Krivorotov, J. A. Katine, V. Tiberkevich, and A. Slavin, Phys. Rev. B **82**, 100410 (2010).

[14] P. K. Muduli, O. G. Heinonen, and J. Åkerman, Phys. Rev. B **83**, 184410 (2011).

[15] See Supplemental Material at http://link.aps.org/supplemental/10.1103/PhysRevLett.108.207203 for additional information.

[16] P. K. Muduli, O. G. Heinonen, and J. Åkerman, J. Appl. Phys. **110**, 076102 (2011).

[17] D. Houssameddine, U. Ebels, B. Dieny, K. Garello, J.-P. Michel, B. Delaet, B. Viala, M.-C. Cyrille, D. Mauri, and J. A. Katine, Phys. Rev. Lett. **102**, 257202 (2009).

[18] H. A. Kramers, Physica (Amsterdam) **7**, 284 (1940); J. van't Hoff, *Etudes de Dynamiques Chimiques* (Muller, Amsterdam, 1884), 4th ed.; S. Arrhenius, Z. Naturforsch. A **4**, 226 (1889).

[19] G. van der Sande, L. Gelens, P. Tassin, A. Scirè, and J. Danckaert, J. Phys. B **41**, 095402 (2008).

[20] S. Beri, L. Gelens, M. Mestre, G. Van der Sande, G. Verschaelt, A. Scirè, G. Mezosi, M. Sorel, and J. Danckaert, Phys. Rev. Lett. **101**, 093903 (2008).

[21] M. Ohtsu, Y. Teramachi, Y. Otsuka, and A. Osaki, IEEE J. Quantum Electron. **22**, 535 (1986).

[22] B. Georges, J. Grollier, V. Cros, A. Fert, A. Fukushima, H. Kubota, K. Yakushijin, S. Yuasa, and K. Ando, Phys. Rev. B **80**, 060404 (2009).

[23] L. Bianchini, S. Cornelissen, J.-V. Kim, T. Devolder, W. van Roy, L. Lagae, and C. Chappert, Appl. Phys. Lett. **97**, 032502 (2010).

[24] V. Tiberkevich, A. Slavin, and J.-V. Kim, Appl. Phys. Lett. **91**, 192506 (2007).

[25] T. Nagasawa, K. Mizushima, H. Suto, K. Kudo, and R. Sato, Appl. Phys. Express **4**, 063005 (2011).